Advantages and limitations of intraoperative ultrasound strain elastography applied in brain tumor surgery: a single-center experience

Santiago Cepeda (cepeda_santiago@hotmail.com)
University Hospital Río Hortega https://orcid.org/0000-0003-1667-8548
Sergio García-García
University Hospital Río Hortega https://orcid.org/0000-0003-2356-5306
Ignacio Arrese
University Hospital Río Hortega
María Velasco-Casares
University Hospital Río Hortega
Rosario Sarabia
University Hospital Río Hortega https://orcid.org/0000-0003-2576-7518

Research Article

Keywords: brain tumor, ultrasound, elastography

Posted Date: June 25th, 2021

DOI: https://doi.org/10.21203/rs.3.rs-654010/v1

Version of Record: A version of this preprint was published at Operative Neurosurgery on March 8th, 2022. See the published version at https://doi.org/10.1227/ons.0000000000000122.

Abstract

Objective Strain elastography is an intraoperative ultrasound (ioUS) modality currently under development with various potential applications in neurosurgery. However, certain technical aspects and limitations have not yet been adequately explained. The objective of our work is to share the experience of our center in a case series of operated brain tumors in which we have applied strain elastography.

Methods We retrospectively analyzed patients who underwent craniotomy for a brain tumor between March 2018 to March 2021. Cases with an ioUS strain elastography study were included. The elastograms were processed semi-quantitatively by decomposing the image in HSB (Hue, Saturation, Brightness) format. Subsequently, the mean tissue elasticity (MTE) values were calculated from the histogram of intensities of the pixels of the hue images. The tumor was manually segmented, and regions of interest (ROIs) were placed in the peritumoral area. An analysis was performed to correlate the histopathological groups and the tumor and peritumoral MTE values using the Kruskal-Wallis test. In addition, a classification model was developed using an algorithm based on a decision tree. Then, model predictive capacity was evaluated through 10-folds cross-validation. Finally, elastogram's quality was assessed to discuss possible sources of artifacts and weaknesses of the ultrasound technique.

Results One hundred two patients with the following histopathological diagnosis were analyzed: 43 high-grade gliomas, 11 low-grade gliomas, 28 meningiomas, and 20 metastases. The tumor MTE values were significantly different between the histopathological groups, $p < .001$, $c^2 = 46.34$, $e^2 = .45$. There were also significant differences for the MTE values concerning the peritumor, $p < .001$, $c^2 = 25.47$, $e^2 = .25$. The decision tree classifier showed an area under the curve (AUC) of the average over classes of 0.97, and the classification accuracy (CA) was 86%. After 10-folds cross-validation, the AUC was 0.73, and the CA was 72%. The main technical limitations found in our series were: the presence of artifacts after dural opening, the variability of the frequency and amplitude of the mechanical pulsations, and the challenge in evaluating deep lesions.

Conclusion ioUS strain elastography is a fast and versatile technique that provides relevant information to adapt the surgical strategy. Furthermore, the stiffness of the tissues has a plausible histopathological correlation. For these reasons, this technique has enormous potential to be exploited in the coming years.

Introduction

Intraoperative ultrasound (ioUS) has recently proven to be a valuable tool within the neurosurgical armamentarium.[22, 23, 30] Its versatility and low cost makes it an optimal intraoperative imaging technique that can be used in almost any center.

In recent years, improvements in image quality, the incorporation of new ultrasound modalities and the possibility of integrating magnetic resonance imaging (MRI) through navigated ultrasound have fostered a resurgence of this technique, gaining followers in the last years.[4, 34, 40] ioUS competes directly with other intraoperative imaging techniques such as intraoperative MRI which has shown significant benefits in brain tumor surgery.[17, 42] However, due to its high economic and infrastructure costs, it cannot be implemented in most centers in middle and low-income countries.

Even though ultrasound is an operator-dependent technique, this characteristic that might be considered a weakness, is really a strength since, in the hands of experienced surgeons, it becomes a great help thanks to its dynamic nature. Its speed of acquisition and its ability to provide information with visual-spatial characteristics that other imaging techniques cannot offer.

Other ultrasound modalities such as contrast-enhanced ultrasound (CEUS), and elastography give a bonus to this imaging technique, leaving its potential still to be fully exploited.[20, 26, 29]

Tissue stiffness assessed by palpation for diagnosis of neoplasms has been used for several years. Ultrasound elastography has been recently developed to display information about tissue stiffness through images.[2, 24, 35] Its use is widespread in other surgical specialties, and shows an incremental application in neurosurgery.[11, 31, 32, 39, 41] In brain tumors, elasticity/stiffness contributes to surgical planning, but this physical property may also be related to the histology and aggressiveness of the tumors.[7, 13] If we add advanced image processing techniques and algorithms based on artificial intelligence, the capacity of this modality opens a new line of research yet to be developed.

The present study aims to share our experience in the performance, interpretation and analysis of ioUS strain elastography in brain tumors, in recent years. Furthermore, we wish to highlight the most relevant technical aspects, the technique's main limitations, and future perspectives. Thus, those who intend to start their application can find solid support elements that facilitate the use and expansion of this promising imaging technique.

Methods

Patient selection

A retrospective analysis was carried out of patients diagnosed with brain tumors consecutively operated in our center between March 2018 and March 2021. Patients with an ioUS study, including the strain elastography modality were selected. Stereotactic biopsies and those cases in which, due to artifacts or failures during their acquisition, the ioUS image quality was inadequate to ensure its processing were discarded. In addition, conventional clinical, demographic, and radiological variables were recorded. In all cases, the patient's written consent was obtained, in addition to the approval of the ethics committee of our center and following the Strengthening the Reporting of Observational Studies in Epidemiology (STROBE) guidelines.

Intraoperative ultrasound image acquisition technique

All cases underwent craniotomy, ensuring that its dimensions were sufficient for the placement and maneuverability of the ultrasound probe. In all cases, we used microsurgical technique, neuronavigation and ultrasonic aspirator. Fluorescence with 5 - aminolevulinic acid was used when a high-grade tumor was suspected. Intraoperative neurophysiological monitoring and cortical-subcortical mapping in awake patients were implemented according to the tumor location.

The first ultrasound image acquisition was performed after craniotomy and before dural opening. Our ultrasound equipment was a Hitachi Noblus model with a C42 micro convex probe at a frequency range of 4–8 MHz, scan width of 20 mm radius and 80 º field of view scan angle. The probe was protected with double sterile sheets, and a minimum amount of conductive gel was used inside the sheet.

The probe was placed on the dural surface, first acquiring B-mode images to visualize the main features of the tumor and their relationships with the surrounding structures. So its morphology, limits, presence of cystic areas, calcifications, etc., were assessed.

Afterward, the strain elastography was performed. The probe was kept in a perpendicular position to the dura, in orthogonal planes in which the largest tumor diameter could be seen. Since biological tissue deforms in a non-linear manner, pre-compression should be minimal with the probe held lightly in contact with the dura.[3] Strain images are produced by using the probe to apply constant gentle pressure toward the brain. The consequent tissue displacement is tracked between pairs of echo frames and strain computed from the axial gradient of the displacements. Under an equal quantity of stress, a stiff region encounters less strain (deformation) than surrounding softer tissue. As a guide for constant pulses, the ultrasound scanner gives a scale indicating the optimal stress, providing real-time feedback to the examiner on the degree and uniformity of the compression technique. The most valuable frames for evaluating strain images with an excellent signal-noise ratio are those with a steady rate of displacement, that is, during the time of downward or upward movement of the transducer.[16] The ultrasound screen simultaneously displays the B-mode image and a color map translucently superimposed on the conventional B-mode image, called elastogram. The color scale ranges from red (soft) to blue (hard). A regular color pattern obtained in several consecutive frames indicates a reliable technique. Quantitative elasticity measurements cannot be achieved, as the local amount of stress is unknown. Thus, strain elastography is a qualitative method in which relative stiffness differences are displayed. During surgery and at the end of it, B-mode images are acquired exclusively to control the resection. All images were stored in DICOM (Digital Imaging and Communications in Medicine) format for further processing.

Elastogram processing

Because the information from the strain images is purely qualitative, semi-quantitative analysis was carried out to transform the colorimetric scale into a dimensionless scale of values called mean tissue elasticity (MTE). The MTE is calculated from the histogram of intensities of the pixels and expressed in arbitrary units.[18, 25] To perform this analysis, the elastograms were

converted to HSB (hue-saturation-brightness) format using the ImageJ software version 1.8.0 (National Institutes of Health, Bethesda, Maryland, USA). The new scale uses the hue images with values ranging from 0 blue-hard to 256 red-soft.

All elastograms with abundant artifacts and void areas were discarded, and three images were selected for each patient on which tumor segmentation and elasticity measurements were performed.

Always taking B-mode as a reference, the tumor was manually segmented using the free-hand tool of ImageJ to create the regions of interest (ROIs). Three circular ROIs with a diameter of 20 pixels were also created for the peritumor, placed in the areas of alteration of echogenicity surrounding the tumor area. Placement was relatively straightforward for meningiomas, metastases, and high-grade gliomas, all of which have a well-defined tumor border. In the cases of low-grade tumors, as there was no clear border between tumor and peritumor, the border areas between echogenicity alterations and the adjacent healthy parenchyma were considered as peritumor. Figure 1.

Finally, the MTE values of the tumor and peritumor are obtained by calculating an average between the three elastograms used for each patient.

Statistical analysis

The distribution of the quantitative variables was evaluated using the Kolmogorov-Smirnov test. The comparison between the histopathological groups and their MTE values in the tumor and peritumoral region was carried out using the Kruskal-Wallis test, applying the epsilon squared coefficient to measure the effect size. Finally, posthoc comparisons were made using Dunn's test with Holm's correction.

A classification model was also developed using three classes or categories: glioma, meningioma, and metastases. In addition, the MTE values of the tumor and peritumoral region were included in the model. A decision tree was used as a classification algorithm. Decision trees are nonparametric methods that do not require assumptions about the distribution of variables within each class. For the first division of the sample into two parts, the feature with the most significant relevance is used, then each node contains a decision criterion based on a single feature. This procedure is repeated until no more divisions are possible. The advantages of decision trees are their simple structure, ease of interpretation and visualization. The classification algorithm is applied to the total sample and then validated through a 10-fold cross-validation process. Basic statistics were carried out with R version 4.0.5 (R Foundation for Statistical Computing, Vienna, Austria), and the decision tree was elaborated with Orange version 3.28.0 (University of Ljubljana, Slovenia).[15]

Results

During the study period, one hundred fifty patients with a diagnosis of brain tumor were operated. Of these, forty patients were discarded because they did not have an intraoperative ultrasound study. Furthermore, eight patients were not included because they had poor quality intraoperative ultrasound images, making their interpretation and analysis impossible.

Thus, 102 patients met the selection criteria. Histopathological diagnoses were: 43 high-grade gliomas, 11 low grade-gliomas, 28 meningiomas and 20 metastases. The characteristics of each group and other clinical and demographic variables are shown in Table 1.

There were no complications related to the intraoperative imaging technique, and the postoperative infection rate was 4.9 %.

The tumor MTE values were significantly different between histopathological groups, $p < .001$, $\chi^2 = 46.34$, $\varepsilon^2 = .45$. Thus, high-grade gliomas were characterized by showing a softer pattern with MTE values of 79.3 (19.3), followed by low-grade gliomas with 88.7 (13.7) and metastases with 114 (29.2). Finally, meningiomas exhibited a significantly higher stiffness than the above tumor mentioned groups, with MTE values of 120 (30.9).

There were also significant differences for the MTE values regarding the peritumor, $p < .001$, $\chi^2 = 25.47$, $\varepsilon^2 = .25$. Thus, in high-grade gliomas [93.2 (25.5)] and low-grade gliomas [91.6 (19.6)], the peritumoral region shows lower stiffness values compared to meningiomas [126 (31.9)] and metastases [122 (37.3)]. Figure 2 and Table 2.

Among the histological types of gliomas, tumor MTE values had the following distribution: astrocytoma grade II = 94.2 (20.8), anaplastic astrocytoma grade III = 73.7 (6.5), oligodendroglioma grade II = 80.2 (3.3), anaplastic oligodendroglioma grade III = 73.7 (6.5) and glioblastoma = 84 (18.4). On the other hand, the following peritumoral MTE values were obtained: astrocytoma grade II = 94.8 (11.1), anaplastic astrocytoma grade III = 101 (25.9), oligodendroglioma grade II = 83.7 (17.6), anaplastic oligodendroglioma grade III = 121 (16.70) and glioblastoma = 89.3 (18.5). No significant differences were found between these groups.

The classifier decision tree was applied with a pruning technique of at least two instances in leaves and at least five instances in each node with a maximum depth of 5. It is a binary tree with stop splitting when reaching 95% of the instances. In the total sample, the area under the curve (AUC) of the average over classes was 0.97, and the classification accuracy (CA) was 86%. After 10-folds cross-validation, the AUC of the average over classes was 0.73 and CA of 72%. A summary of the results is shown in Table 3, Fig. 3 and Supplemental Figs. 1 and 2.

Discussion

In the present study, we demonstrate that ioUS strain elastography is a safe and easy-to-apply technique. Furthermore, through the semi-quantitative analysis of the elastograms, it is possible to characterize the different tumor types based on the calculated values of MTE.

Among the strengths of our study, we can mention that this is the largest published series about the application of ioUS strain elastography in brain tumor surgery. In addition, we confirm the findings of an initial study of our group in which we applied and validated the semi-quantitative analysis technique of the colorimetric scale of the elastograms to obtain a measure of the stiffness of the tissues.[7] As far as we know, we are pioneers in applying this type of ultrasound image analysis in brain pathology.

Among the limitations of our work, we can mention the lack of external validation of the elastogram acquisition technique. Furthermore, in our series of cases, the images were acquired by a single surgeon (S.C.). Therefore, in future work, an evaluation of the reproducibility of the acquisition of images must be carried out. Despite this, we offer a detailed description of the ultrasound technique to be replicated in future studies.

Elastogram quality

The image quality of ultrasound images and elastograms is susceptible to multiple factors.[1, 34, 36] The ultrasound equipment used in our series requires gentle mechanical compressions to acquire strain images. However, other ultrasound scanners are capable of generating elastograms using spontaneous brain pulsations.[27, 28] To obtain high-quality images, the elastograms are acquired before the dural opening. The dura mater offers resistance, and thanks to its elastic capacity, it is possible to perform more homogeneous pulsations, which translates into more uniform elastograms and fewer signal voids. Figure 4. In those cases in which small dural tears occurred, the quality of the elastogram did not vary significantly, at least in a qualitative way. Figure 5A-B. These variations should be studied in the future.

Regarding the ROI size, strain elastography demonstrates the relative stiffness of tissue, so it is crucial to include enough normal tissue surrounding the tumor. The most suitable image quality was registered in phantom experiments when the lesion of interest covered 25–50 % of the ROI.[19] Caution must be taken when using a convex probe since the region immediately in the middle of the transducer could apply more stress than the lateral portions of the probe, producing a “lateral stiffness artifact”.[5]

Another factor that influences the quality of the image is the presence of cystic areas. Figure 5C. The interposition of liquid content can seriously influence the transmission of mechanical pulsations. In these cases, the penetration of mechanical waves does not occur homogeneously throughout the tissue to be explored. Measuring displacement between two frames solely detects random noise, which is displayed in different ways. A commonly described artifact is the BGR (blue-green-red) sign encountered in small cystic tumors. Large cystic lesions are more likely to be seen as "black holes".[14] This circumstance occurs especially in metastases and less frequently in high-grade gliomas, possibly due to their content (cystic-mucinous or necrotic).

Elastograms can also vary depending on the tumor's location and, therefore, on how the mechanical impulse spreads. For example, in deep-seated tumors, the distance from the probe to the tumor can produce artifactual images and overestimate its stiffness. Figure 5D. In addition, in those cases of tumors of the skull base or posterior fossa, the mechanical impulse can make the tissue collide against bone structures, altering its compressibility and, consequently, the elastographic image. Also, it is recommendable to avoid assessment of tissue near stiff areas, as soft tissue will undergo more strain when it is above hard tissue.

Meningiomas

In meningioma surgery, strain elastography permits addressing the resection of the tumor with reliable information about its stiffness. The presence of a cleavage plane and the relationships with surrounding neurovascular structures allow the surgeon to adapt the surgical technique and anticipate the extent of the resection. This utility has been demonstrated in previous works.[6, 21, 27] In addition, they are a tumor group in which the elastograms are usually relatively homogeneous because they generally behave as compact masses.

Gliomas

The elastographic pattern of gliomas is very characteristic from a qualitative and quantitative point of view. They are usually tumors softer than the surrounding brain parenchyma, with extensive involvement of the peritumoral white matter, which also shows less stiffness. Peritumoral infiltration may explain a change in elasticity in these regions, as has been postulated.[10, 31] On the other hand, the contrast of the color image is superior to the B-mode when establishing the tumor's edges, as reported by Selbekk et al. in his work.[33]

Metastases

Metastases also tend to be softer than the normal parenchyma. However, the stiffness of the white matter does not appear to be significantly different compared to that found in primary tumors. Possibly, the presence of pure vasogenic edema present in metastases and meningiomas could explain this difference in peritumoral elasticity. For this, it is essential in future studies to carry out a histopathological correlation of these areas.

Histological classification based on elastography and glioma grading

Our results show significant differences in tumor and peritumoral stiffness expressed through MTE between gliomas and the rest of the tumor groups (metastases and meningiomas). These results are validated by applying the classification algorithm based on a decision tree, which reaches a precision of 70%. However, even though metastases showed less tumor stiffness than meningiomas (113 vs. 120), these differences were not statistically significant. Furthermore, their peritumoral MTE values were very similar (122 vs. 126).

Regarding glioma grading by ioUS elastography, we found previous descriptions in the literature in which a lower elasticity was observed in high-grade gliomas than low-grade gliomas.[7, 13, 28, 43] However, in our study, although tumor and peritumoral MTE values are indeed lower in high-grade glioma than low-grade glioma (80 vs. 86, 91 vs. 96, respectively), these differences were not statistically significant. Neither, we found differences after analyzing the histological subtypes and degrees of aggressiveness in the glioma group.

Strain elastography versus shear wave elastography

There are two types of ultrasound elastography, strain and shear wave. Strain elastography is a qualitative technique and provides knowledge on the relative stiffness between one tissue and another. Shear wave elastography (SWE) is a quantitative method that offers an estimated value of the tissue stiffness that can be expressed in either the shear wave speed through the tissues in meters per second or converted to Young’s modulus and expressed in kilopascals.[16] A critical advantage of SWE is to perform acquisitions to assess the extent of the resection. Using strain elastography, it is impossible to perform compressions on the deformed parenchyma and the interposition of fluid that fills the surgical cavity. In this sense, the SWE stands as the best option to assess residual tumor.[12]

The main limitation of the SWE is the size of the Q-box, which is the region of interest in which the color maps and elasticity values are obtained. Unfortunately, this region is usually limited in size, and the vast majority of cases do not cover the entire tumor and peritumor area. In this regard, strain elastography has an advantage by offering a more extensive and visually richer image compared to SWE. In addition, strain elastography allows an overview of relative tissue stiffness in a large field of view. This aspect is advantageous if we want to assess, for example, the stiffness of a tumor area close to a noble structure and to know globally if its stiffness has a homogeneous or heterogeneous pattern.

Each technique has its advantages and disadvantages, and maybe they should be used in a complementary way in brain tumor surgery.

Brain elastography and future perspectives

The usefulness of intraoperative cerebral elastography goes beyond the characterization of the histopathological types and serves as a support for surgical resection. Knowledge of the elasticity and stiffness of tissues is biologically based and is related to the cytoarchitecture of tumors and their ability to infiltrate in gliomas.[37, 38]

Advanced image processing techniques, such as texture analysis, also known as radiomics, can increase the diagnostic potential of this imaging technique and even contribute to predict the survival and progression of primary brain neoplasms.[9]

On the other hand, image processing automation and the combination of recognition techniques based on artificial intelligence are yet to be explored in depth.[8]

Conclusion

Our experience on brain tumor's ioUS transmitted through this series of cases allows us to confirm the applicability of strain elastography in brain tumor surgery. In addition, this technique provides relevant information for surgical planning and differentiation of the different tumor types. Its potential is still under development, but it is already emerging as a valuable neurosurgical tool for the upcoming years.

Declarations

Disclosures:

This research did not receive any specific grant from funding agencies in the public, commercial, or not-for-profit sectors.

Conflicts of Interest:

The authors report no conflict of interest concerning the materials or methods used in this study or the findings specified in this paper.

Funding:

No funding was received for this research.

Acknowledgments:

We thank Santiago Aja-Fernández, Professor at the ETSI (Higher Technical School of Telecommunications Engineering) and (LPI) Image Processing Laboratory, at the University of Valladolid, for his technical assistance in planning our study.

References

1. Altieri R, Melcarne A, Di Perna G, et al (2018) Intra-Operative Ultrasound: Tips and Tricks for Making the Most in Neurosurgery. Surg Technol Int 33:353–360
2. Bamber J, Cosgrove D, Dietrich C, et al (2013) EFSUMB Guidelines and Recommendations on the Clinical Use of Ultrasound Elastography. Part 1: Basic Principles and Technology. Ultraschall der Medizin - Eur J Ultrasound 34(02):169–184
3. Barr RG, Zhang Z (2012) Effects of precompression on elasticity imaging of the breast: development of a clinically useful semiquantitative method of precompression assessment. J Ultrasound Med 31(6):895–902
4. Del Bene M, Perin A, Casali C, Legnani F, Saladino A, Mattei L, Vetrano IG, Saini M, DiMeco F, Prada F (2018) Advanced Ultrasound Imaging in Glioma Surgery: Beyond Gray-Scale B-mode. Front Oncol. doi: 10.3389/fonc.2018.00576
5. Bilgen M, Insana MF (1997) Error analysis in acoustic elastography. II. Strain estimation and SNR analysis. J Acoust Soc Am 101(2):1147–54
6. Cepeda S, Arrese I, García-García S, Velasco-Casares M, Escudero-Caro T, Zamora T, Sarabia R (2020) Meningioma Consistency Can Be Defined by Combining the Radiomic Features of Magnetic Resonance Imaging and Ultrasound Elastography. A Pilot Study Using Machine Learning Classifiers. World Neurosurg. doi: 10.1016/j.wneu.2020.11.113
7. Cepeda S, Barrena C, Arrese I, Fernandez-Pérez G, Sarabia R (2020) Intraoperative Ultrasonographic Elastography: A Semi-Quantitative Analysis of Brain Tumor Elasticity Patterns and Peritumoral Region. World Neurosurg 135:e258–e270
8. Cepeda S, García-García S, Arrese I, Fernández-Pérez G, Velasco-Casares M, Fajardo-Puentes M, Zamora T, Sarabia R (2021) Comparison of Intraoperative Ultrasound B-Mode and Strain Elastography for the Differentiation of Glioblastomas From Solitary Brain Metastases. An Automated Deep Learning Approach for Image Analysis. Front Oncol. doi: 10.3389/fonc.2020.590756
9. Cepeda S, García-García S, Arrese I, Velasco-Casares M, Sarabia R (2021) Relationship between the overall survival in glioblastomas and the radiomic features of intraoperative ultrasound: a feasibility study. J Ultrasound. doi: 10.1007/s40477-021-00569-9
10. Cepeda S, García-García S, Velasco-Casares M, Fernández-Pérez G, Zamora T, Arrese I, Sarabia R (2021) Is There a Relationship between the Elasticity of Brain Tumors, Changes in Diffusion Tensor Imaging, and Histological Findings? A Pilot Study Using Intraoperative Ultrasound Elastography. Brain Sci 11(2):271
11. Chakraborty A, Berry G, Bamber J, Dorward N (2006) Intra-operative Ultrasound Elastography and Registered Magnetic Resonance Imaging of Brain Tumours: A Feasibility Study. Ultrasound 14(1):43–49
12. Chan HW, Uff C, Chakraborty A, Dorward N, Bamber JC (2021) Clinical Application of Shear Wave Elastography for Assisting Brain Tumor Resection. Front Oncol 11:619286
13. Chauvet D, Imbault M, Capelle L, Demene C, Mossad M, Karachi C, Boch A-L, Gennisson J-L, Tanter M (2016) In Vivo Measurement of Brain Tumor Elasticity Using Intraoperative Shear Wave Elastography. Ultraschall Med 37(6):584–590
14. Cho N, Moon WK, Chang JM, Kim SJ, Lyou CY, Choi HY (2011) Aliasing artifact depicted on ultrasound (US)-elastography for breast cystic lesions mimicking solid masses. Acta Radiol 52(1):3–7
15. Demšar J, Curk T, Erjavec A, et al (2013) Orange: Data Mining Toolbox in Python. J Mach Learn Res 14(1):2349–2353
16. Dietrich CF, Barr RG, Farrokh A, Dighe M, Hocke M, Jenssen C, Dong Y, Saftoiu A, Havre RF (2017) Strain Elastography - How To Do It? Ultrasound Int open 3(4):E137–E149
17. Garcia-Garcia S, García-Lorenzo B, Ramos PR, et al (2020) Cost-Effectiveness of Low-Field Intraoperative Magnetic Resonance in Glioma Surgery. Front Oncol 10:586679
18. Gheonea DI (2010) Real-time sono-elastography in the diagnosis of diffuse liver diseases. World J Gastroenterol 16(14):1720
19. Havre RF, Elde E, Gilja OH, Odegaard S, Eide GE, Matre K, Nesje LB (2008) Freehand real-time elastography: impact of scanning parameters on image quality and in vitro intra- and interobserver validations. Ultrasound Med Biol 34(10):1638–50
20. Kearns KN, Sokolowski JD, Chadwell K, Chandler M, Kiernan T, Prada F, Kalani MYS, Park MS (2019) The role of contrast-enhanced ultrasound in neurosurgical disease. Neurosurg Focus 47(6):E8
21. Menna G, Olivi A, Della Pepa GM (2021) Integration of Different Intraoperative Ultrasound Modalities in Meningioma Surgery: A 4-Step Approach. World Neurosurg 146:376–378

22. Moiyadi A V (2016) Intraoperative Ultrasound Technology in Neuro-Oncology Practice-Current Role and Future Applications. World Neurosurg 93:81–93
23. Munkvold BKR, Jakola AS, Reinertsen I, Sagberg LM, Unsgård G, Solheim O (2018) The Diagnostic Properties of Intraoperative Ultrasound in Glioma Surgery and Factors Associated with Gross Total Tumor Resection. World Neurosurg 115:e129–e136
24. Ophir J, Céspedes I, Ponnekanti H, Yazdi Y, li X (1991) Elastography: A quantitative method for imaging the elasticity of biological tissues. Ultrason Imaging 13(2):111–134
25. Orlacchio A, Bolacchi F, Antonicoli M, Coco I, Costanzo E, Tosti D, Francioso S, Angelico M, Simonetti G (2012) Liver Elasticity in NASH Patients Evaluated with Real-Time Elastography (RTE). Ultrasound Med Biol 38(4):537–544
26. Della Pepa GM, Ius T, La Rocca G, et al (2020) 5-Aminolevulinic Acid and Contrast-Enhanced Ultrasound: The Combination of the Two Techniques to Optimize the Extent of Resection in Glioblastoma Surgery. Neurosurgery 86(6):E529–E540
27. Della Pepa GM, Menna G, Stifano V, et al (2021) Predicting meningioma consistency and brain-meningioma interface with intraoperative strain ultrasound elastography: a novel application to guide surgical strategy. Neurosurg Focus 50(1):E15
28. Prada F, Del Bene M, Rampini A, et al (2019) Intraoperative Strain Elastosonography in Brain Tumor Surgery. Oper Neurosurg 17(2):227–236
29. Prada F, Perin A, Martegani A, et al (2014) Intraoperative contrast-enhanced ultrasound for brain tumor surgery. Neurosurgery 74(5):542–52; discussion 552
30. Sastry R, Bi WL, Pieper S, Frisken S, Kapur T, Wells W, Golby AJ (2017) Applications of Ultrasound in the Resection of Brain Tumors. J Neuroimaging 27(1):5–15
31. Scholz M, Noack V, Pechlivanis I, Engelhardt M, Fricke B, Linstedt U, Brendel B, Schmieder K, Ermert H, Harders A (2005) Vibrography during tumor neurosurgery. J Ultrasound Med 24(7):985–992
32. Selbekk T, Bang J, Unsgaard G (2005) Strain processing of intraoperative ultrasound images of brain tumours: Initial results. Ultrasound Med Biol 31(1):45–51
33. Selbekk T, Brekken R, Indergaard M, Solheim O, Unsgård G (2012) Comparison of contrast in brightness mode and strain ultrasonography of glial brain tumours. BMC Med Imaging 12(1):11
34. Selbekk T, Jakola AS, Solheim O, Johansen TF, Lindseth F, Reinertsen I, Unsgård G (2013) Ultrasound imaging in neurosurgery: approaches to minimize surgically induced image artefacts for improved resection control. Acta Neurochir (Wien) 155(6):973–980
35. Sigrist RMS, Liau J, Kaffas A El, Chammas MC, Willmann JK (2017) Ultrasound elastography: Review of techniques and clinical applications. Theranostics 7(5):1303–1329
36. Šteňo A, Buvala J, Babková V, Kiss A, Toma D, Lysak A (2021) Current Limitations of Intraoperative Ultrasound in Brain Tumor Surgery. Front Oncol 11:659048
37. Stewart DC, Rubiano A, Dyson K, Simmons CS (2017) Mechanical characterization of human brain tumors from patients and comparison to potential surgical phantoms. PLoS One 12(6):e0177561
38. Tsitlakidis A, Aifantis EC, Kritis A, Tsingotjidou AS, Cheva A, Selviaridis P, Foroglou N (2020) Mechanical properties of human glioma. Neurol Res 42(12):1018–1026
39. Uff CE, Garcia L, Fromageau J, Dorward N, Bamber JC (2009) Real-time ultrasound elastography in neurosurgery. 2009 IEEE Int. Ultrason. Symp. IEEE, pp 467–470
40. Unsgaard G, Selbekk T, Brostrup Müller T, Ommedal S, Torp SH, Myhr G, Bang J, Nagelhus Hernes TA (2005) Ability of navigated 3D ultrasound to delineate gliomas and metastases - Comparison of image interpretations with histopathology. Acta Neurochir (Wien) 147(12):1259–1269
41. Wu D fang, He W, Lin S, Zee CS, Han B (2018) The real-time ultrasonography for fusion image in glioma neurosugery. Clin Neurol Neurosurg 175(October):84–90
42. Yahanda AT, Chicoine MR (2021) Intraoperative MRI for Glioma Surgery: Present Overview and Future Directions. World Neurosurg 149:267–268

43. Yin L, Cheng L, Wang F, Zhu X, Hua Y, He W (2021) Application of intraoperative B-mode ultrasound and shear wave elastography for glioma grading. Quant Imaging Med Surg 11(6):2733–2743

Tables

Table 1. Patient characteristics	
Variable	**n**
Age	60.76 ± 11.61
Sex	
Female	45 (44 %)
Male	57 (66 %)
Histopathology	
Meningiomas	28 (27.4 %)
High-grade gliomas	43 (41.2 %)
Glioblastoma	34
Anaplastic astrocytoma grade III	7
Anaplastic oligodendroglioma grade III	2
Low-grade gliomas	11 (11.8 %)
Astrocytoma grade II	6
Oligodendroglioma grade II	5
Metastases	20 (19.6 %)
Lung	7
Breast	2
Ovarian	4
Gastrointestinal	3
Prostate	2
Urothelial	1
Thyroid	1
Tumor location	
Frontal	47 (46.1 %)
Temporal	22 (21.5 %)
Parietal	21 (20.6 %)
Occipital	5 (4.9 %)
Posterior fossa / cerebellum	7 (6.9 %)
Values are expressed as the mean ± standard deviation or as frequency (%).	

Table 2. Analysis of MTE values of tumor types in their different regions											
REGION	**Descriptive statistics**				**Kruskal-Wallis test**					**Post hoc Dunn test**	
	PATHOLOGY	**n**	**MEDIAN**	**IQR**	**c^2**	**df**	**p**	**e^2**	**95% CI**	**COMPARISON**	**p (Holm)**
TUMOR (MTE)					46.34	3	<.001	.46	.31 - .60	HGG-LGG	.366
	HIGH-GRADE GLIOMA	43	79.3	19.3						HGG-MENINGIOMA	<.001
	LOW-GRADE GLIOMA	11	88.7	13.7						LGG-MENINGIOMA	.009
	MENINGIOMA	28	120	30.9						HGG-METS	<.001
	METASTASES	20	114	29.2						LGG-METS	.130
										MENINGIOMA-METS	.267
PERITUMORAL REGION (MTE)					25.47	3	<.001	.25	.12 - .44	HGG-LGG	.86
	HIGH-GRADE GLIOMA	43	93.2	25.5						HGG-MENINGIOMA	<.001
	LOW-GRADE GLIOMA	11	91.9	19.6						LGG-MENINGIOMA	.011
	MENINGIOMA	28	126	31.9						HGG-METS	.002
	METASTASES	20	122	37.2						LGG-METS	.019
										MENINGIOMA-METS	.905

IQR = interquartile range, df = degrees of freedom, METS = metastases, MTE = mean tissue elasticity, HGG = high-grade glioma, LGG = low-grade glioma.

Table 3. Performance evaluation of the classification model by decision tree algorithm				
Model	**AUC**	**CA**	**Precision**	**Recall**
Training				
Average over classes	0.968	0.863	0.860	0.863
Glioma	0.983	0.933	0.883	0.981
Meningioma	0.978	0.922	0.833	0.893
Metastases	0.932	0.882	0.833	0.500
10-fold Cross Validation				
Average over classes	0.734	0.716	0.702	0.716
Glioma	0.859	0.853	0.831	0.907
Meningioma	0.725	0.765	0.559	0.679
Metastases	0.573	0.814	0.566	0.250
AUC = area under the curve, CA = classification accuracy.				

Figures

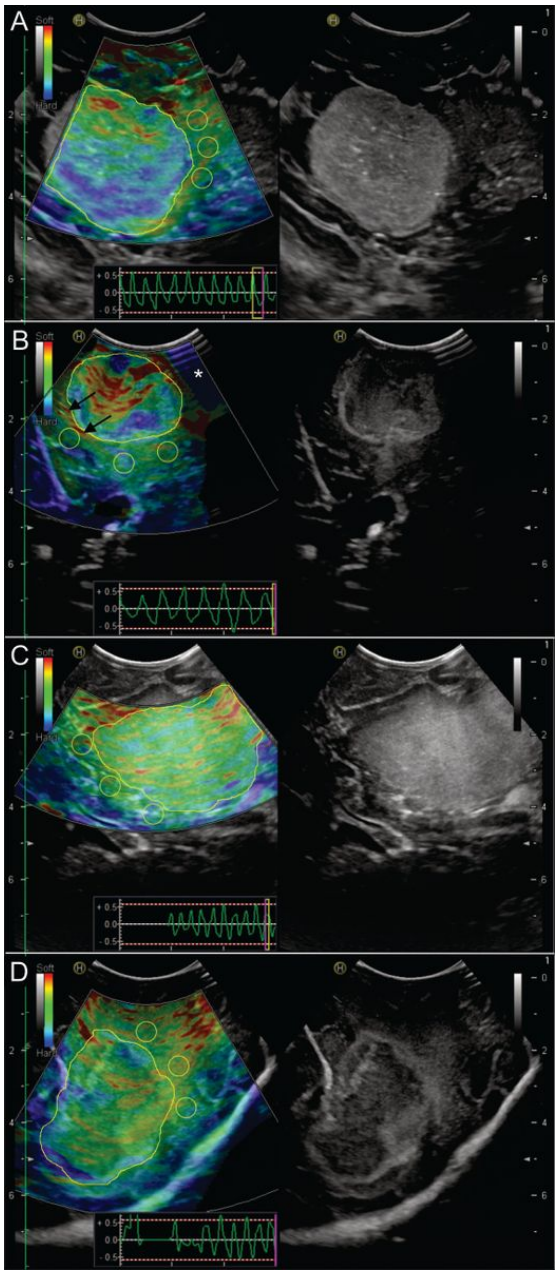

Figure 1

Illustrative cases showing the methodology applied for image analysis. Tumors were manually segmented using the free-hand tool (yellow line). Regions of interest (ROI) were placed over the peritumor area (yellow circles). Elastography (left) and B-mode (right) images of the four tumor categories. A: A frontal meningioma with heterogeneous consistency, stiffer in the peripheral portion of the tumor (capsule) and without a cleavage plane. B: A frontal ovarian metastasis with a more rigid capsule and mucinous content. An arachnoid plane can be identified in its medial border represented by the slip interface (black arrows). A “lateral stiffness artifact” (white asterisk) can also be identified. C: An insular WHO grade II astrocytoma. Tumor limits are challenging to be delineated. However, strain image shows a slightly better contrast compared to B-mode. D: A frontal glioblastoma showing soft homogeneous consistency. Although tumor borders can be distinguished, the peritumoral region also shows a low elasticity pattern.

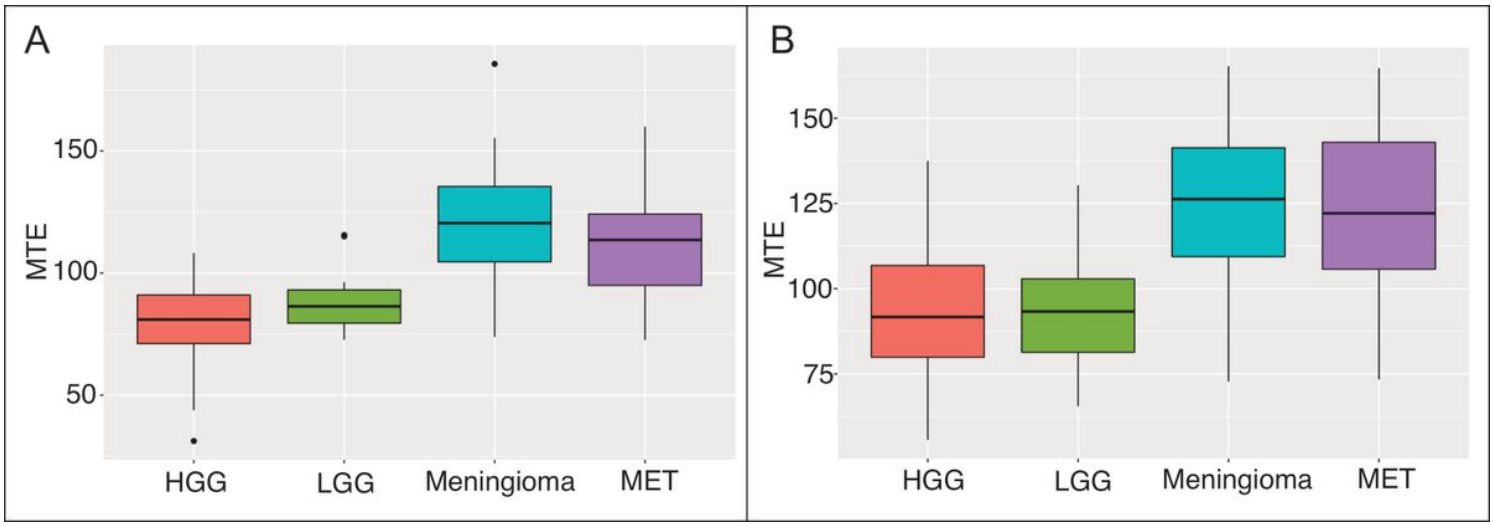

Figure 2

Box plots showing differences in the median mean tissue elasticity (MTE) values of tumor (left) and peritumoral (right) regions according to the histopathological groups: Low-grade gliomas (LGG), high-grade gliomas (HGG), meningiomas and metastases (MET).

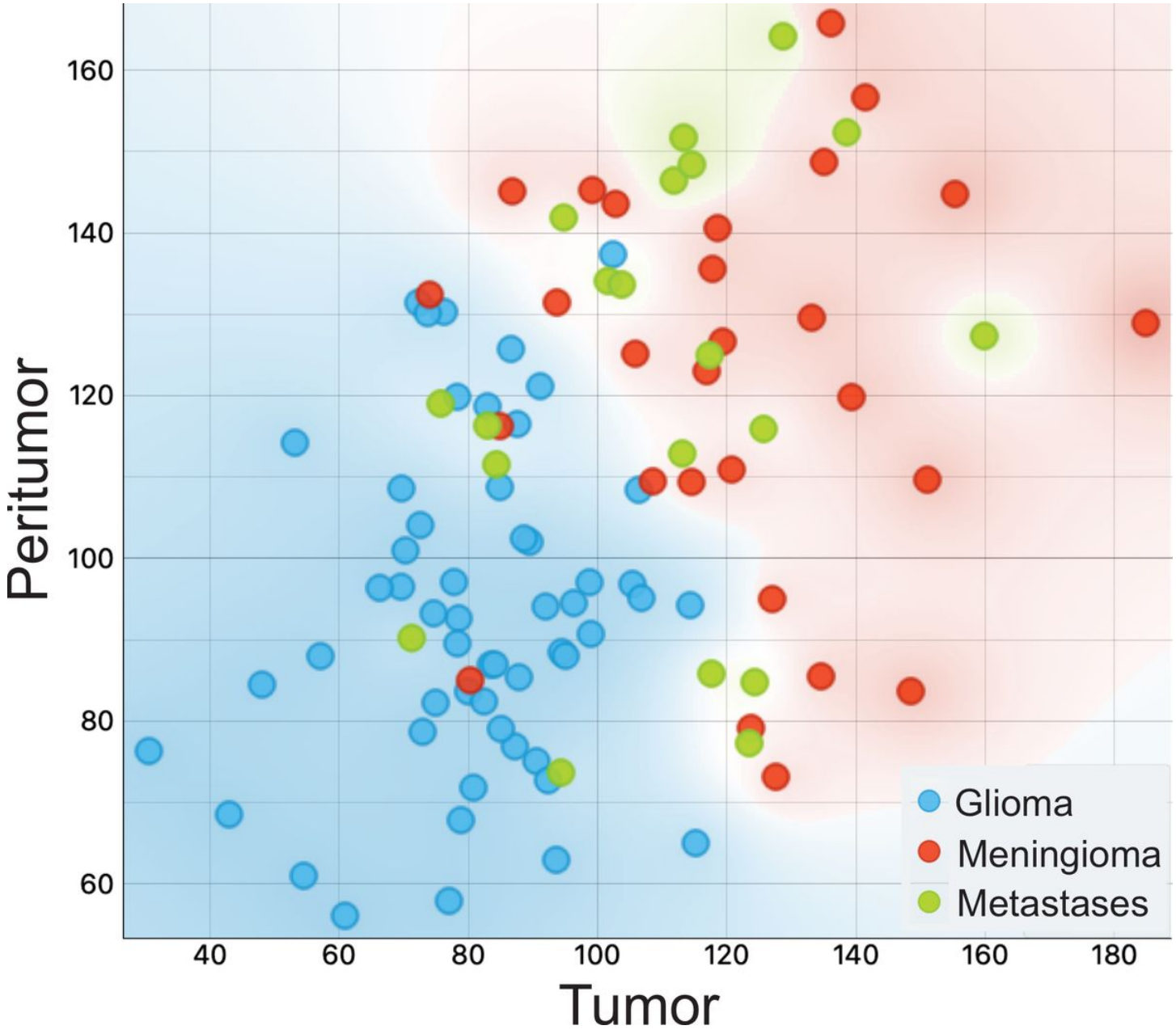

Figure 3

Scatter plot showing the classification of instances by the decision tree based on the mean elasticity (MTE) values of tumor and peritumoral region. Gliomas (blue circles) are located in the left lower portion of the plot, while meningiomas (red circles) appear in the right upper corner because they show higher MTE values. Metastases (green circles) exhibit a diverse representation in the plot without a predominant distribution.

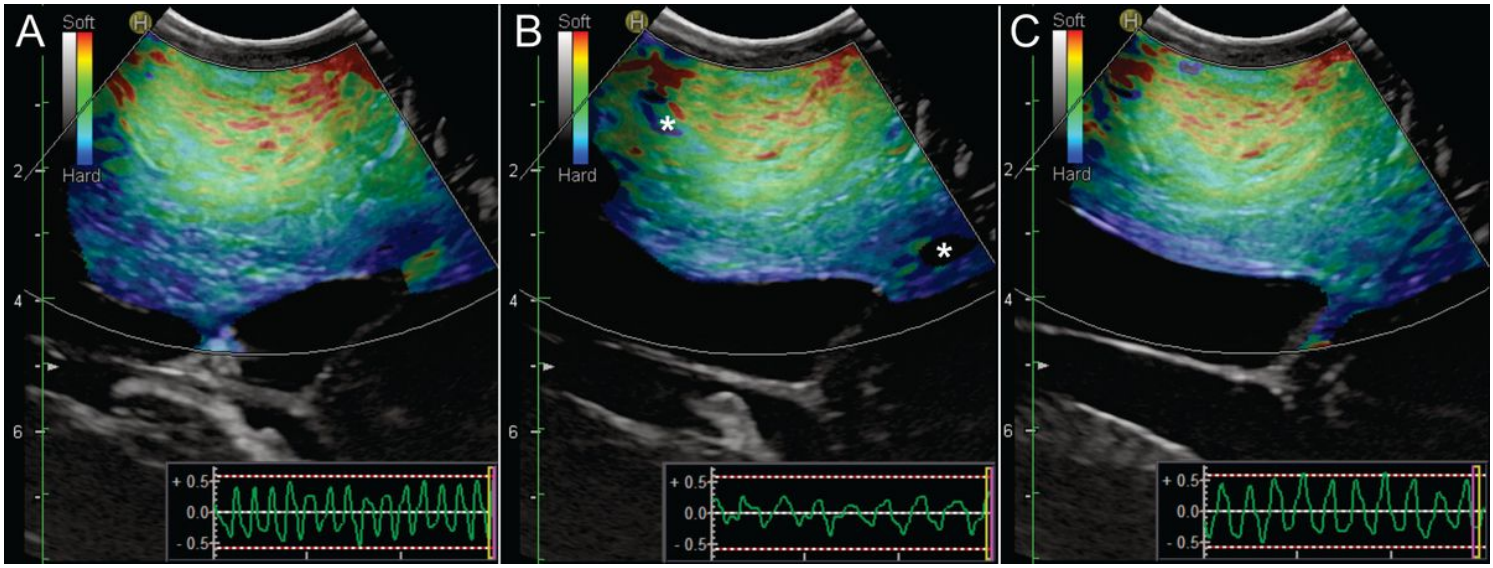

Figure 4

Examples of modifications in the elastograms by different types of compressions. In the right lower corner of each image, the ultrasound scanner shows a graph in a unit-less scale from -5 to +5 representing the frequency and amplitude of manual compressions. A: high-frequency pulses affect the quality of deeper zones, producing heterogeneous images. B: Slower compression with less amplitude can produce elastograms with black zones (white asterisk). C: Regular compressions with a constant amplitude generate the best quality elastograms.

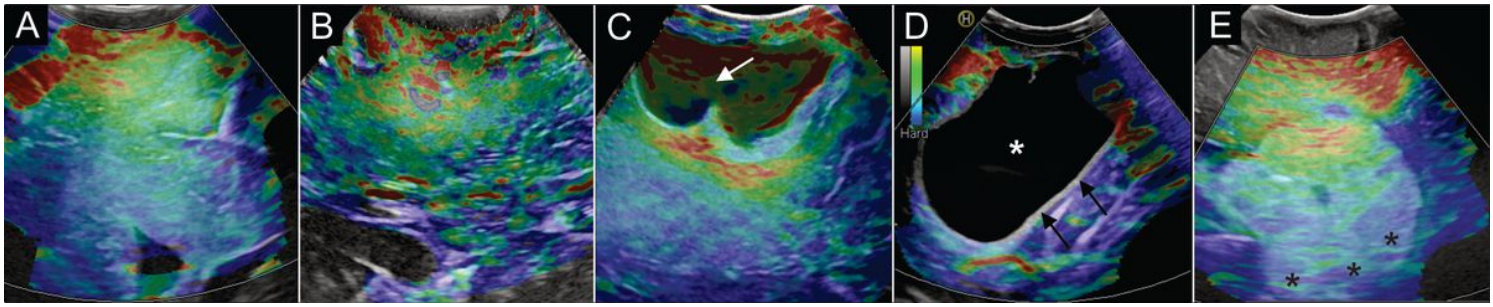

Figure 5

Illustrative cases of artifactual images. A: In this low-grade frontal glioma, small dural tears can produce artifacts in the superficial zone, but the remaining quality of the elastogram is not significantly affected. B: An insular low-grade glioma showing an elastogram altered with many empty zones and a heterogenous pattern due to the acquisition of images was performed after dural opening or through deformed brain parenchyma. C: A small cystic metastsis showing the BGR (blue-green-red) artifact (white arrow). D: Large cystic metastasis impedes the propagation of the mechanical pulse. As a result, the elastogram shows zones without strain information (black arrows) in the tumor capsule and black zones (white asterisk) over the cyst. E: An intraventricular meningioma showing a good quality of the elastogram in the most superficial portion of the tumor. However, in the deeper portion of the tumor crossing the midline (black asteriks), the elastogram show a fake stiffness that the intraoperative surgeon's perception couldn't confirm.

Supplementary Files

This is a list of supplementary files associated with this preprint. Click to download.

- supplementarydata.docx